European Review for Medical and Pharmacological Sciences 2020; 24: 4232-4245

Long noncoding RNA LINC00511 promoted cell proliferation and invasion *via* regulating miR-124-3p/EZH2 pathway in gastric cancer

H.-G. HUANG[1,2], X.-L. TANG[3], X.-S. HUANG[2], L. ZHOU[2], Y.-G. HAO[4], Y.-F. ZHENG[5]

[1]The First Clinical Medical College of Jinan University, Guangzhou, Guangdong, China
[2]Department of Gastroenterological Surgery, the Affiliated Hospital of Youjiang Medical University for Nationalities, Baise, Guangxi Zhuang Autonomous Region, China
[3]Malignant Tumor TCM "Yi Qi Qing Du" Key Research Office, Jiangxi Institute of Traditional Chinese Medicine, Nanchang, Jiangxi, China
[4]Department of Rehabilitation, Shanghai Putuo People's Hospital, Shanghai, China
[5]Department of Oncology, Zhujiang Hospital of Southern Medical University, Guangzhou, Guangdong, China

Haige Huang and *XiaoLing Tang* contributed equally to this work

Abstract. – OBJECTIVE: Growing evidence has shown that long non-coding RNAs (lncRNAs) can serve as prospective markers for survival in patients with gastric cancer (GC). In this study, we mainly focused on the potential roles of LINC00511 in the development process of GC.

PATIENTS AND METHODS: RT-PCR was used to detect the expressions of LINC00511 and miR-124-3p in GC tumor tissues, adjacent tissues and GC cell lines. Furthermore, correlations between LINC00511 with miR-124-3p, and miR-124-3p with EZH2, were analyzed by Correlation analysis. Moreover, the overall survival (OS) of patients was analyzed using Kaplan-Meier method. Additionally, proliferation ability was measured by CCK-8 assay and invasion ability of GC cell line was detected by transwell assay. Besides, Western blot was performed to measure protein levels of GC tissues and GC cell lines. Finally, Dual-Luciferase reporter assay was performed to prove the potential binding sites between LINC00511 and miR-124-3p, miR-124-3p and EZH2.

RESULTS: We found that LINC00511 was significantly increased in GC tissues and GC cell lines, which was associated with tumor growth, metastasis and predicted poor diagnosis of GC patients. MiR-124-3p was decreased in GC tissues and GC cell lines, which was negatively correlated with LINC00511 and EZH2. Furthermore, EZH2 was increased in GC tissues and GC cell lines, which was positively correlated with LINC00511. Moreover, LINC00511 inhibition repressed cell proliferation and invasion in MKN28 cells, the protein levels of Cyclin D1, ICAM-1, VCAM-1 and N-cadherin were repressed, while E-cadherin was increased. Besides, Luciferase gene reporter assay indicated that LINC00511 could sponge with miR-124-3p, which could directly target at EZH2, an oncogenic gene. We found that miR-124-3p/EZH2 axis regulated cell proliferation and invasion in MKN28 cells. Finally, the inhibited cell proliferation and invasion abilities were eliminated following with miR-124-3p inhibition in MKN28 cells with LINC00511 knockdown.

CONCLUSIONS: According to the results, we found that LINC00511 was increased in GC tissues, which was associated with the poor OS in patients with GC. We uncovered a previously unappreciated LINC00511/miR-124-3p/EZH2 signaling axis in promoting cell proliferation and invasion in GC patients and GC cell lines, which suggested that it might be a potential target for treating human GC.

Key Words:
LINC00511, MiR-124-3p, EZH2, Progression and invasion, Gastric cancer.

Introduction

Gastric cancer (GC) is a malignant cancer in the digestive system. Its incidence and mortality rank both top five in the world[1-3]. Thanks to the novel therapeutic treatments and diagnosis methods during past years, the mortality is slowly decreasing and future survival is slowly improving

Corresponding Author: Yanfang Zheng, MD; e-mail: drzhengyf@sina.com

for GC patients[1-4]. However, the future outcomes for patients are not yet satisfied, most patients are suffering with pain and many of them are in later stage. We need to find new methods for early-stage diagnosis and develop more novel therapies and targets for treating with GC.

Long non-coding RNAs (lncRNAs) do not encode proteins, but they have the capacity to regulate different functions in normal development of human body and in various diseases[5-8]. It has been found that lncRNAs are critical regulators in the development of cancers[9-11], including GC[12-14]. LINC00511 has been found to be increased and it was regarded as an oncogene in some human cancers[15-17]. Yu et al[17] reported it promote tumor cell proliferation, motility and improve the malignancy in cervical cancer[17]. Deng et al[15] found that LINC00511 could promote the malignant phenotype in renal cell carcinoma; Lu et al[16] showed that LINC00511 contributed to tumor formation and stemness in breast cancer by interacting with miR-185-3p, etc. However, whether LINC00511 plays some roles in GC remained unclear.

MicroRNAs (miRNAs) are short RNAs that also do not encode proteins, but they still have the capacity to regulate different functions by binding with 3' untranslated regions (UTR) of target genes in various diseases[18-21]. Studies revealed that lncRNAs could function as a competing endogenous RNA (ceRNA) to interact with miRNA[22,23] and regulate the development of different cancers[24,25]. MiR-124-3p was reported to be a tumor suppressor in several human cancers[26-28], such as bladder cancer[26], endometrial cancer[27] and breast cancer[28]. MiR-124-3p was reduced in GC and then promoted tumor growth[29,30]; however, the detailed mechanisms in GC remained not fully understood.

In this study, we investigated the expressions of LINC00511 in GC tumor tissues and we found that it was significantly increased in GC tissues and GC cell lines; therefore, we explored the potential functions of LINC00511 in GC patients.

Patients and Methods

Patients

80 patients with GC were included, tumor tissues and their corresponding adjacent non-tumor tissues were collected by surgical resection in our hospital from Jul 2013 to Oct 2014. All samples were frozen at -80°C. Patients age ranged from 40 to 72 years old, 52 cases of male and 28 cases of female; 43 cases of tumor size ≤ 5 cm, 27 cases of tumor size ≥ 5 cm; 36 cases with lymph node metastasis. Clinical parameters in GC patients were showed in Table I. This investigation was approved by the Faculty of Medicine's Ethics Committee of our hospital and informed consent was obtained from all patients.

Cell Culture

Human normal gastric epithelial cell (GES-1) and GC cell lines, including MGC, HGC, MKN25, MKN28 were purchased from the American Type Culture Collection (ATCC, Manassas, VA, USA). Cells were cultured in Dulbecco's

Table I. The relationships between LINC00511 and clinical parameters in GC patients

Parameters	Low LINC00511 (n = 40)	High LINC00511 (n = 40)	*p*-value
Age			0.335
< 60Y	25	30	
≥ 60Y	15	10	
Sex			0.482
Male	28	24	
Female	12	16	
Tumor size			
< 5 cm	32	21	**0.017**
≥ 5 cm	8	19	
TNM stage			
I-II	29	17	**0.012**
III-IV	11	23	
Lymph node metastasis			
Yes	13	23	**0.042**
No	27	17	
Distant metastasis			
Yes	12	24	**0.013**
No	28	16	

Modified Eagle's Medium (DMEM; Invitrogen, Carlsbad, CA, USA), which were supplemented with 10% fetal bovine serum (FBS; Gibco, Grand Island, NY, USA), 100 U/ml penicillin (HyClone, South Logan, UT, USA) and 100 μg/ml streptomycin (HyClone, South Logan, UT, USA). All cells were cultured in an appropriate incubator at the condition of 37°C with 5% CO_2.

Construction of Lentivirus and Cell Transfection

The short hairpin RNA (shRNA) of LINC00511 or shRNA of EZH2 and negative control (NC) were provided by Invitrogen (Carlsbad, CA, USA) and were cloned into different lentivirus (Invitrogen, Carlsbad, CA, USA), which resulted with LINC00511 or EZH2 inhibition. LV-sh-LINC00511 or LV-shEZH2 and LV-NC were respectively infected into MKN28 cells for 24 hours. Then, a stable cell line of MKN28 with LINC00511 inhibition or EZH2 inhibition was obtained after 1 to 2 weeks. Indicated cells were seeded in 6-well plates (1×10^6/well) until 70%, miR-124-3p inhibitor or miR- NC was transfected into MKN28 cells with the transfection reagent Lipofectamine 2000 (Invitrogen, Carlsbad, CA, USA) according to its instructions. Cells were harvested at the indicated time point for further study.

RNA Extraction and Quantitative Real-Time PCR

TRIzol reagent (Invitrogen, Carlsbad, CA, USA) was used for total RNA extraction from human tissues and cell lines according to the protocol. PrimeScript™ RT reagent Kit (TaKaRa, Dalian, China) was used to perform the reverse transcription according to the protocol. PCR primers were synthesized by Gene Pharma (Shanghai, China) and sequences were listed in Table II. SYBR Premix Ex Taq II (TaKaRa, Dalian, China) was used to detect mRNA expressions, which were normalized to GAPDH or U6 and $2^{-\Delta\Delta CT}$ method was used to calculate relative gene expressions. Three independent experiments were repeated to get the mean value.

Cell Counting Kit-8 (CCK-8) Assay

Cell proliferation abilities of GC cells were tested using CCK8 assay (Dojindo, Kumamoto, Japan) according to the protocol. 0.25% trypsin was used to digest MKN28 cells, which were then seeded on 96-well plates (2×10^3 cells/ml) and cultured in the incubator. For each well, 10 μl CCK-8 agent was added after cultivating for 1 d, 2 d and 3 d. Finally, the optical density (OD) value was recorded at 450 nm with microplate reader (Thermo Fisher Scientific, Waltham, MA, USA) and cell. Each group was set with three replicate wells and three independent experiments were repeated to get the mean value.

Flow Cytometric Analysis of Cell Cycle

MKN28 cells were washed twice by phosphate-buffered saline (PBS) and then were digested with trypsin, cell precipitation was collected after centrifugation. 75% ethanol was added into the precipitation at 4°C for 4 h, which was washed twice by PBS, then cell pellet was stained with FITC-Annexin V and Propidium Iodide (PI) at 25°C for 10 mins. Finally, the stained cells were subjected to a FACSCalibur system (BD Pharmingen, Franklin Lakes, NJ, USA) to measure the cell cycle status. Three independent experiments were repeated to get the mean value.

Transwell Assay

Cell invasion ability was evaluated by transwell assay and transwell chambers (BD Biosciences, Franklin Lakes, NJ, USA) were pur-

Table II. Primer sequences for RT-PCR.

Genes	Primer sequences
LINC00511	Forward: 5'-CGCAAGGACCCTCTGTTAGG-3' Reverse: 5'-GAAGGCGGATCGTCTCTCAG-3'
miR-124-3p	Forward: 5'-TGTGATGAAAGACGGCACAC-3' Reverse: 5'-CTTCCTTTGGGTATTGTTTGG-3'
EZH2	Forward: 5'-AACACCAAACAGTGTCCATGCT-3' Reverse: 5'-CTAAGGCAGCTGTTTCAGAGAG-3'
GAPDH	Forward: 5'-GGAGTCCACTGGTGTCTTCA-3' Forward: 5'-GGGAACTGAGCAATTGGTGG-3'
U6	Forward: 5'-CGCTTCGGCAGCACATATACT-3' Forward: 5'-CGCTTCACGAATTTGCGTGTC-3'

chased. Cells (4×10^4 cell/well) of each group were added into the top of chamber on the non-coated membrane, and 20% fetal bovine serum (FBS) was added into lower chamber. Then, indicated cells were put in the upper chamber for 24 h. The cells which still remained on the upper chamber were wiped out using cotton swabs, while the invasive cells on the other side were fixed and stained with 95% methanol for 10 mins and stained with 0.5% crystal violet (Beyotime, Shanghai, China). Finally, light microscope (Olympus Corporation, Tokyo, Japan) was used to observe the invaded cells. Three independent experiments were repeated to get the mean value.

Protein Extraction and Western Blot

Tissue samples and cells were extracted using a radioimmunoprecipitation assay (RIPA) protein extraction reagent buffer (Sigma-Aldrich, St. Louis, MO, USA) with a protease inhibitor (Roche, Basel, Switzerland), followed by detection of protein concentrations using a bicinchoninic acid assay (BCA) kit (Pierce Chemical Co., Rockford, IL, USA). 30 mg protein of each sample was added onto 10% sodium dodecyl sulphate-polyacrylamide gel electrophoresis (SDS-PAGE) and the separated proteins were transferred onto polyvinylidene difluoride (PVDF) membranes, which were blocked with skim milk at room temperature for 1 h. Then, membranes were incubated with primary antibodies overnight at 4°C. Primary antibodies were obtained from Abcam (Abcam, Cambridge, MA, USA), EZH2 (1:2000, 85 kDa), Cyclin D1 (1:2000, 33 kDa), ICAM-1 (1:3000, 95 kDa), VCAM-1 (1:3000, 100 kDa), N-cadherin (1:1000, 100 kDa), E-cadherin (1:1000, 110 kDa) and GAPDH (1:5000, 36 kDa). Then, membranes were incubated with matched secondary antibodies (1:5000) for 1 h. Finally, protein bands were visualized by adding SuperSignal® ECL Kit (Thermo Fisher Scientific, Waltham, MA, USA) in enhanced chemiluminescence (ECL) detection system (Thermo Fisher Scientific, Waltham, MA, USA).

Luciferase Assay

The wild type potential binding sequences and mutant sequences of LINC00511 or EZH2 were synthesized into pmiR-GLO (Promega, Madison, WI, USA), named wt-LINC00511, mut-LINC00511, mt-EZH2 and mut-EZH2. Cells were seeded in 48-well plates and cultured for 12 h and then cells were transfected with 4 ng *Renilla* Luciferase vector and 200 ng firefly Luciferase plasmids for 24 h. Next, they were respectively co-transfected with 200 ng plasmids with wt-LINC00511, mut-LINC00511, mt-EZH2 or mut-EZH2. After 24 h, miR-124-3p mimic or miR-NC was respectively transfected into wild type plasmids and mutant plasmids for another 24 h. Finally, cells were lysed, and Luciferase activities were measured using Dual-Luciferase Reporter Assay System (Promega, Madison, WI, USA). Data were normalized to *Renilla* Luciferase activity and the relative activities of Luciferase were calculated.

Statistical Analysis

All data were analyzed by SPSS 18.0 (SPSS Inc., Chicago, IL, USA) and GraphPad Prism 6.0 (La Jolla, CA, USA). Statistical significance between groups was analyzed by Student's *t*-test or one-way ANOVA and SNK method. Count data were analyzed by chi-square test. Correlations in human GC tissues and adjacent tissues were analyzed using Pearson's correlation analysis. Overall survival of GC patients was analyzed by Kaplan-Meier survival test. Three independent experiments were repeated to get the mean value. If $p<0.05$, it was considered statistically significant.

Results

LINC00511 Was Highly Expressed In GC Tissues and GC Cell Lines

To investigate the roles of LINC00511 in GC, RT-PCR was used to detect mRNA expressions of LINC00511 in 80 paired GC tissues and non-tumor tissues. Results showed that LINC00511 was significantly increased in GC tissues, compared with non-tumor tissues (Figure 1A) ($p<0.001$). Furthermore, we analyzed the correlation between LINC00511 expression and clinicopathological features in patients with GC. Results showed that the LINC00511 upregulation was correlated with advanced TNM stage, metastasis and tumor size (Table I) ($p<0.05$). Moreover, LINC00511 in patients of stage III-IV was significantly increased, compared to that of stage I-II (Figure 1B) ($p<0.001$). We also found that LINC00565 expression in GC tissues larger than 5 cm was much higher than those less than 5 cm (Figure 1C) ($p<0.001$). Besides, LINC00511 in patients with metastasis was much higher than

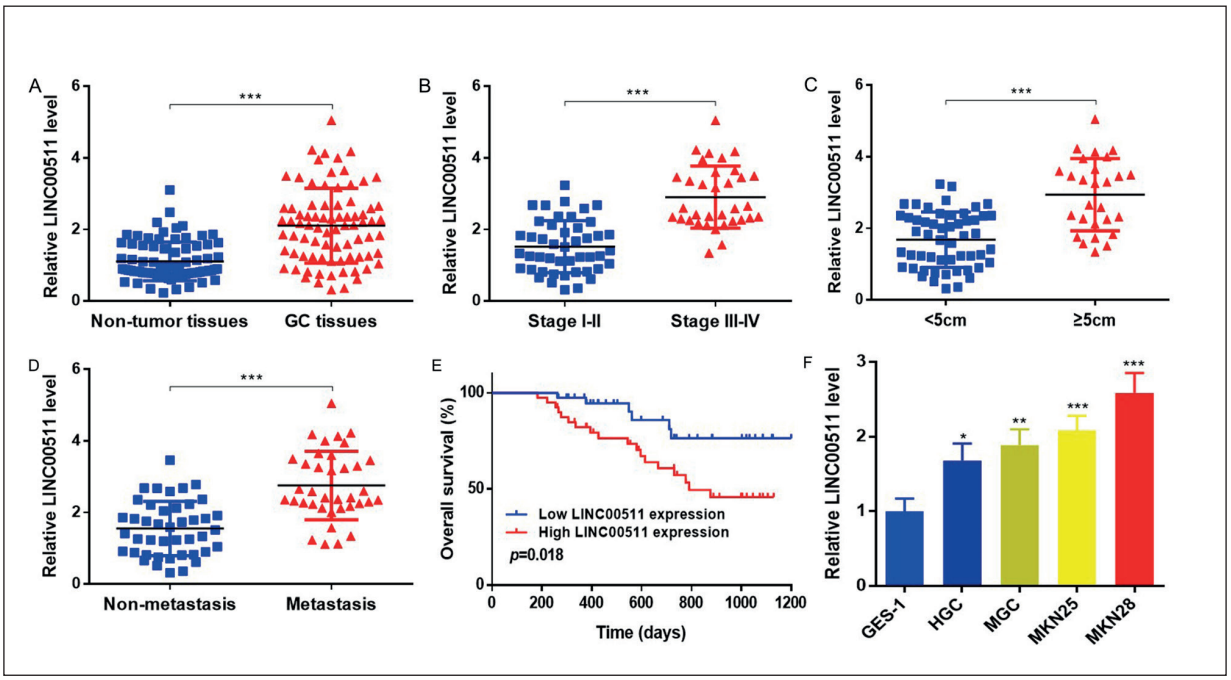

Figure 1. LINC00511 was highly expressed in GC tissues and GC cell lines. **A,** RT-qPCR was used to detect LINC00511 expressions in GC tissues (n=80) and adjacent non-tumor tissues (n=80). **B,** LINC00511 expressions in GC patients of stage I-II (n=46) and stage III-IV (n=34) were analyzed. **C,** LINC00511 expressions in GC tissues larger than 5 cm (n=53) and less than 5 cm (n=26) were analyzed. **D,** LINC00511 expressions in GC patients with metastasis (n=37) and non-metastasis (n=43) were analyzed. **E,** Kaplan-Meier survival analysis was performed to analyze the OS in LINC00511 low expression and high expression group. **F,** RT-qPCR was used to detect LINC00511 expressions in GC cell lines. *p<0.05; **p<0.01, ***p<0.001.

those without metastasis (Figure 1D) (p<0.001). In addition, Kaplan-Meier survival analysis revealed that GC patients with LINC00511 upregulation had a lower overall survival (OS) than the low expression group (Figure 1E) (p<0.05). Additionally, we found that LINC00511 expressions were significantly increased (Figure 1F) (p<0.05). Collectively, these data suggested that LINC00511 was increased in GC tissues, which was correlated with metastasis, tumor size and the poor diagnosis of GC patients. However, the roles and mechanism of LINC00511 in GC remained unknown.

LINC00511 Knockdown Inhibited Cell Proliferation and Invasion In MKN28 Cells

To explore the functions of LINC00511 in GC, LINC00511 sh-RNA was constructed and cloned into a lentiviral (LV-sh LINC00511), resulted with LINC00511 inhibition. LV-sh LINC00511 was infected into MKN28 cells, and the results showed that LINC00511 was significantly repressed (Figure 2A) (p<0.001). Then, CCK-8 assay showed that LINC00511 inhibition repressed cell proliferation ability after 3 days, compared with LV-NC (Figure 2B) (p<0.01). Furthermore, flow cytometry (FACS) illustrated that LINC00511 inhibition repressed cell growth by improving cell distribution in G0/G1 phase and reducing cell distribution in S phase (Figure 2C) (p<0.01). Besides, transwell assay demonstrated that LINC00511 inhibition could repress cell invasion ability, compared with p-NC (Figure 2D) (p<0.01). Additionally, WB was performed to detect protein expressions of proliferation associated gene Cyclin D1 and invasion associated genes, including ICAM-1, VCAM-1, N-cadherin and E-cadherin. Results showed that protein levels of Cyclin D1, ICAM-1, VCAM-1 and N-cadherin were repressed, while E-cadherin was promoted (Figure 2E, F) (p<0.01), which indicated that the proliferation and invasion abilities were both repressed. These data suggested that LINC00511 knockdown inhibited cell proliferation and invasion in MKN28 cells.

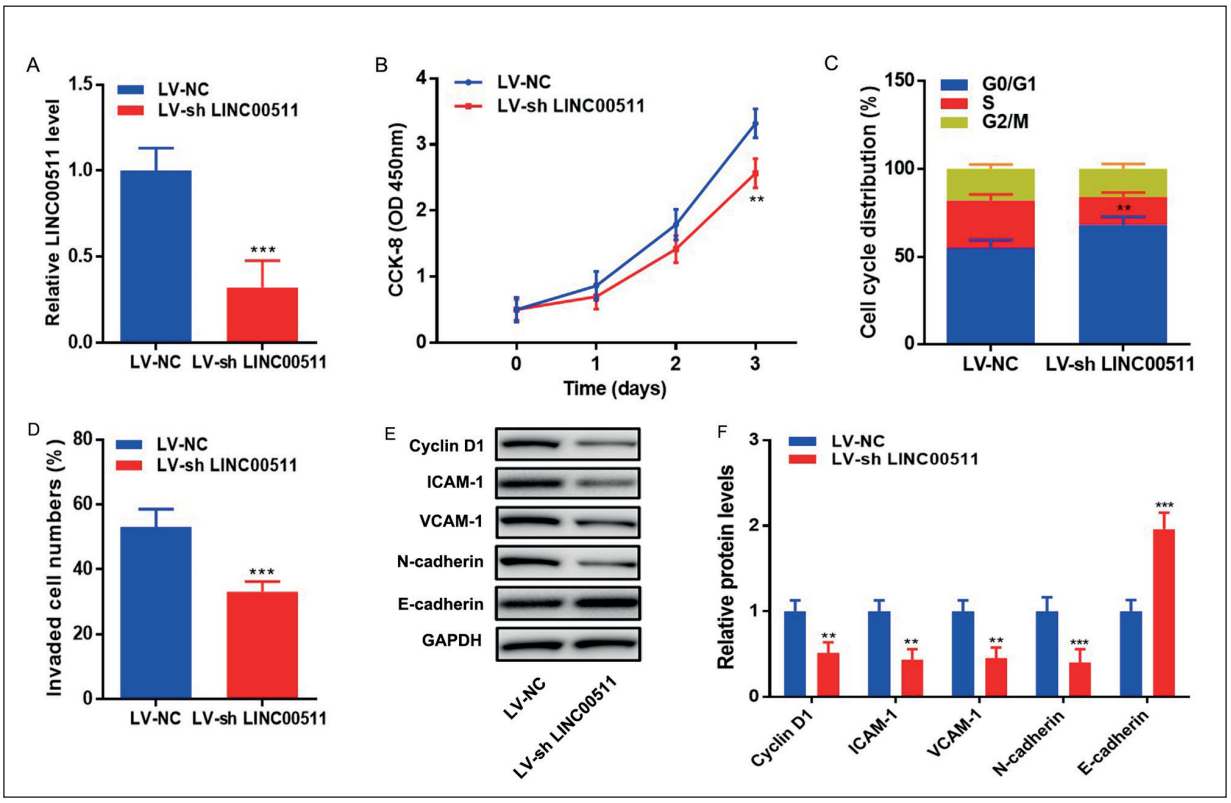

Figure 2. LINC00511 knockdown inhibited cell proliferation and invasion in MKN28 cells. **A,** LINC00511 mRNA expressions were detected after LV-sh LINC00511 or LV-NC infection into MKN28 cells. **B,** Proliferation abilities of indicated cells were measured by CCK8 assay. **C,** Cell cycle distribution was evaluated by FACS. **D,** Invasion abilities were detected by transwell assay. **E, F,** Protein levels of Cyclin D1, ICAM-1, VCAM-1, N-cadherin and E-cadherin were detected by WB (magnifications × 0.8). **p<0.01, ***p<0.001.

LINC00511 Could Directly Sponge With Mir-124-3p In MKN28 Cells

To further explore the mechanism that LINC00511 participated in cell proliferation and invasion in GC, we used bioinformatics analysis to predict the target miRNAs of LINC00511 and we found that miR-124-3p might be a potential target miRNA of LINC00511, which played important roles in biological functions of various cancers[26-28]. Then, we detected the expressions of miR-124-3p in GC tissues and non-tumor tissues. Results revealed that miR-124-3p was significantly repressed in GC tissues (Figure 3A) (p<0.001). Furthermore, miR-124-3p expression in patients at stage III-IV was much lower than patients at stage I-II (Figure 3B) (p<0.001). Moreover, miR-124-3p expression in GC tissues larger than 5 cm was much lower than patients less than 5 cm (Figure 3C) (p<0.001). Besides, miR-124-3p in patients with metastasis was lower than patients with non-metastasis (Figure 3D) (p<0.001). In addition, correlation analysis was performed, and the results revealed that LINC00511 was negatively correlated with miR-124-3p in GC patients (Figure 3E) (p<0.05), especially in patients at the stage of III-IV, patients with tumor size larger than 5 cm and patients with metastasis (Figure 3F-H) (p<0.01). Additionally, we found that the expressions of miR-124-3p were significantly repressed in GC cell lines, especially in MKN28 cells (Figure 3I) (p<0.001) and it was upregulated following with LINC00511 inhibition (Figure 3J) (p<0.001). Collectively, these data illustrated that LINC00511 was negatively interacted with miR-124-3p and it was predicted to be a target for LINC00511 by bioinformatics analysis. To verify whether LINC00511 could competitively bind with miR-124-3p, wild type and mutant sequences of LINC00511 were constructed into GLO vectors (Figure 3K) and the Luciferase reporter assay was performed. Results showed

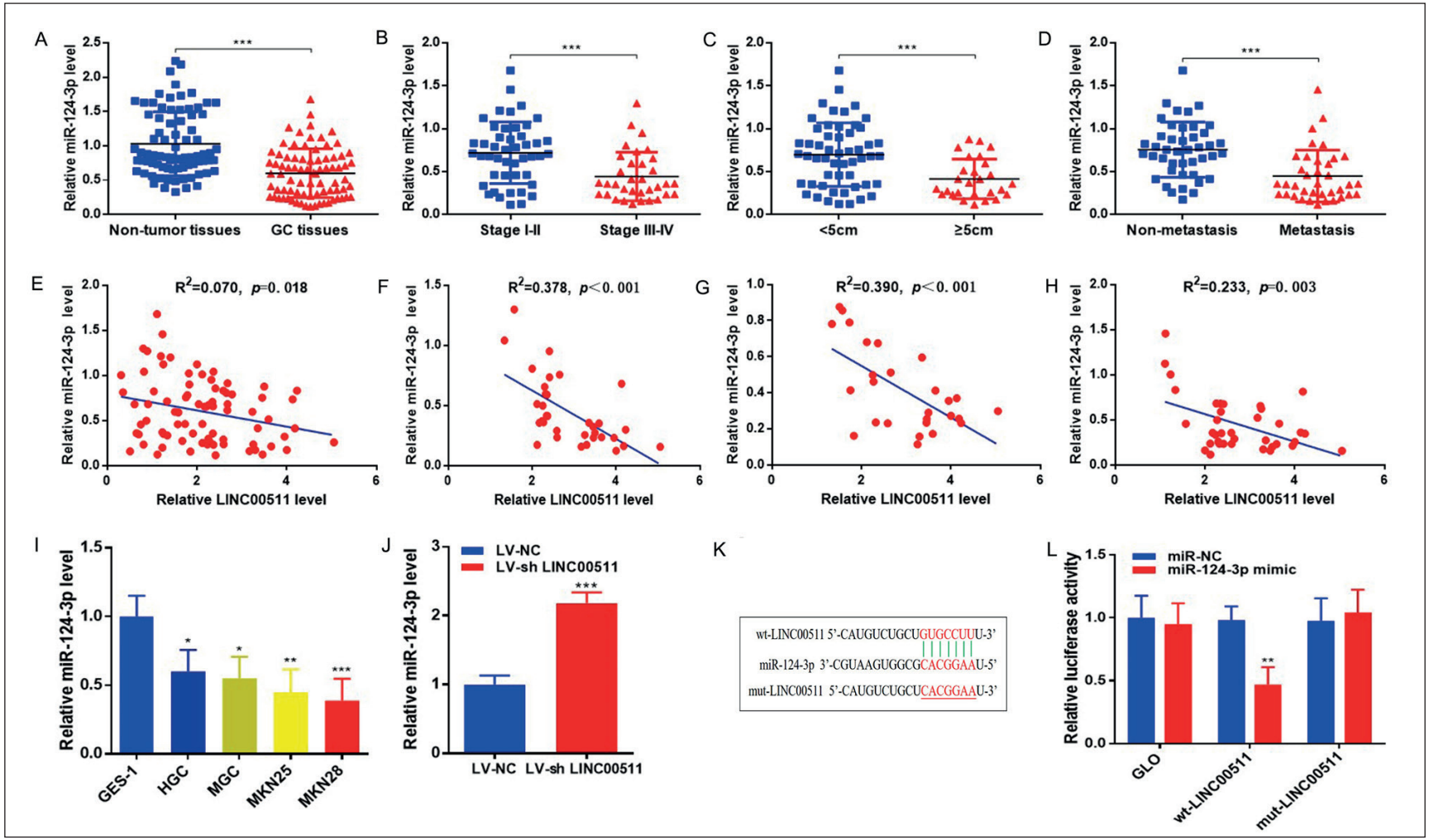

Figure 3. LINC00511 could directly sponge with miR-124-3p in MKN28 cells. **A,** MiR-124-3p expressions in GC tissues (n=80) and adjacent non-tumor tissues (n=80) were detected. **B,** MiR-124-3p expressions in patients with stage I-II (n=46) and stage III-IV (n=34) were analyzed. **C,** MiR-124-3p expressions in GC tissues larger than 5 cm (n=53) and less than 5 cm (n=26) were analyzed. **D,** MiR-124-3p expressions in GC patients with metastasis (n=37) and non-metastasis (n=43) were analyzed. **E-H,** Correlations between LINC00511 and miR-124-3p were analyzed in GC patients, patients at stage III-IV, tumor size larger than 5 cm and patients with metastasis. **I, J,** MiR-124-3p expressions in GC cell lines and MKN28 infected with LV-sh LINC00511 or LV-NC were detected. **K,** Potential wild type and mutant sequences of LINC00511 were constructed. **L,** Luciferase gene reporter assay was performed to verify the binding site in MKN28 cells. *p<0.05, **p<0.01, ***p<0.001.

that relative Luciferase activity in MKN28 cells co-transfected with wt-LINC00511 and miR-124-3p mimic was significantly repressed, while Luciferase activity was reversed in cells co-transfected with mut-LINC00511 and miR-124-3p mimic (Figure 3L) ($p<0.01$). These data demonstrated that LINC00511 was negatively related with miR-124-3p in GC and it could directly bind with miR-124-3p in MKN28 cells.

MiR-124-3p Could Directly Bind With EZH2 In MKN28 Cells

To further investigate how miR-124-3p regulated cell proliferation and invasion in GC, we used Targetscan database to predict target genes of miR-124-3p. EZH2 was predicted as a potential target, which was found to be an oncogenic gene to promote tumorigenesis in some cancers[31-33]. Then, we detected protein expressions of EZH2 in GC tissues and non-tumor tissues. Results revealed that EZH2 was increased in GC tissues (Figure 4A) ($p<0.001$). Furthermore, EZH2 levels in patients at stage III-IV were much higher than patients at stage I-II (Figure 4B) ($p<0.001$). Moreover, EZH2 levels in GC tissues larger than 5 cm were much higher than patients less than 5 cm (Figure 4C) ($p<0.001$) and EZH2 was much higher in patients with metastasis than patients with non-metastasis (Figure 4D) ($p<0.001$). Besides, correlation analysis revealed that EZH2 was negatively correlated with miR-124-3p in GC patients (Figure 4E) ($p<0.05$), especially in patients at the stage of III-IV, patients with tumor size larger than 5 cm and patients with metastasis (Figure 4F-H) ($p<0.01$). Additionally, we found that the protein expressions of EZH2 were upregulated in GC cell lines, especially in MKN28 cells (Figure 4I) ($p<0.001$). Above all, the data showed that EZH2 was negatively interacted with miR-124-3p and it was predicted to be a target for miR-124-3p by Targetscan database. To verify that miR-124-3p could directly bind to EZH2, we synthesized and constructed wild type and mutant binding sequences of EZH2 (Figure 4J). Luciferase reporter assay illustrated that relative Luciferase activity in MKN28 cells co-transfected with wt-EZH2 and miR-124-3p mimic was significantly repressed, while it was reversed in cells co-transfected with mut-LINC00511 and miR-124-3p mimic (Figure 4K) ($p<0.01$). Collectively, these data demonstrated that miR-124-3p could directly bind with EZH2 and repress protein expression in MKN28 cells.

MiR-124-3p/EZH2 Axis Regulated Cell Proliferation and Invasion In MKN28 Cells

To confirm that miR-124-3p/EZH2 axis contributed to regulate cell proliferation and invasion of GC, LV-sh EZH2 was synthesized and constructed, resulting with EZH2 inhibition. LV-sh EZH2 or LV-NC was respectively transfected into MKN28 cells and stable MKN28 cells were selected. Then, miR-124-3p inhibitor and miR-NC were respectively transfected into stable MKN28 cells. Results revealed that mRNA expressions of EZH2 were significantly repressed following with LV-sh EZH2 infection (Figure 5A) ($p<0.001$), while it was improved following with miR-124-3p inhibition (Figure 5A) ($p<0.001$). Furthermore, miR-124-3p was promoted following with EZH2 inhibition, while it was repressed following with miR-124-3p inhibition (Figure 5A) ($p<0.001$). Moreover, CCK-8 assay illustrated that EZH2 inhibition repressed cell proliferation ability, while it was repressed following with miR-124-3p inhibition (Figure 5B) ($p<0.01$). FACS assay showed that EZH2 inhibition repressed cell growth by improving cell distribution in G0/G1 phase and reducing cell distribution in S phase, while it was reversed following with miR-124-3p inhibition (Figure 5C) ($p<0.01$). Transwell assay demonstrated that EZH2 inhibition repressed cell invasion ability, while it was promoted following with miR-124-3p inhibition (Figure 5D) ($p<0.01$). Additionally, WB showed that EZH2 inhibition repressed protein expressions of Cyclin D1, ICAM-1, VCAM-1 and N-cadherin, while they were reversed following with miR-124-3p inhibition (Figure 5E,F) ($p<0.01$). These data suggested that miR-124-3p/EZH2 axis regulated cell proliferation and invasion in MKN28 cells.

LINC00511 Was Positively Interacted With EZH2

We have demonstrated that miR-124-3p was a target for LINC00511 and it could directly bind with EZH2. To further understand the relationship between LINC00511 and EZH2, correlation analysis was performed. Results showed that EZH2 was positively correlated with LINC00511 in GC patients (Figure 6A) ($p<0.05$), as well as positively correlated with LINC00511 in GC patients at stage of III-IV, patients with tumor size larger than 5 cm and patients with metastasis (Figure 6B-D) ($p<0.01$). Furthermore, we found that EZH2 was repressed following with LINC00511 inhibition in EZH2 cells (Figure 6E) ($p<0.01$). These data indicated that LINC00511 was positively inter-

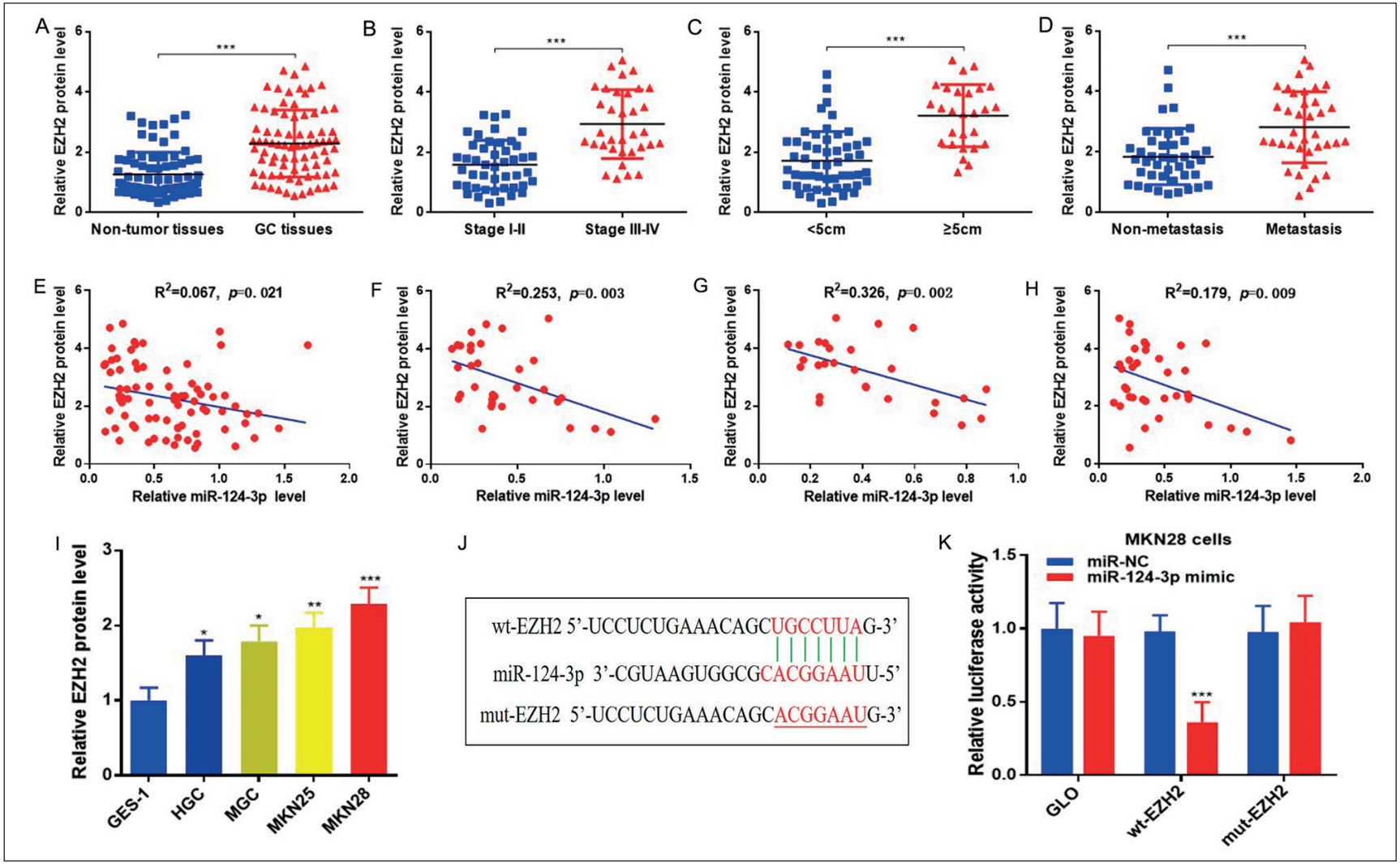

Figure 4. MiR-124-3p could directly bind with EZH2 in MKN28 cells. **A,** EZH2 protein expressions in GC tissues (n=80) and non-tumor tissues (n=80) were detected. **B,** EZH2 protein expressions in patients with stage I-II (n=46) and stage III-IV (n=34) were analyzed. **C,** EZH2 protein expressions in GC tissues larger than 5 cm (n=53) and less than 5 cm (n=26) were analyzed. **D,** EZH2 protein expressions in GC patients with metastasis (n=37) and non-metastasis (n=43) were analyzed. **E-H,** Correlations between EZH2 and miR-124-3p were analyzed in GC patients, patients at stage III-IV, tumor size larger than 5 cm and patients with metastasis. **I,** EZH2 protein expressions in GC cell lines were detected. **J,** Potential wild type and mutant binding sequences of EZH2 were constructed. **K,** Luciferase gene reporter assay was performed to verify the binding site in MKN28 cells. **p*<0.05, ***p*<0.01, ****p*<0.001.

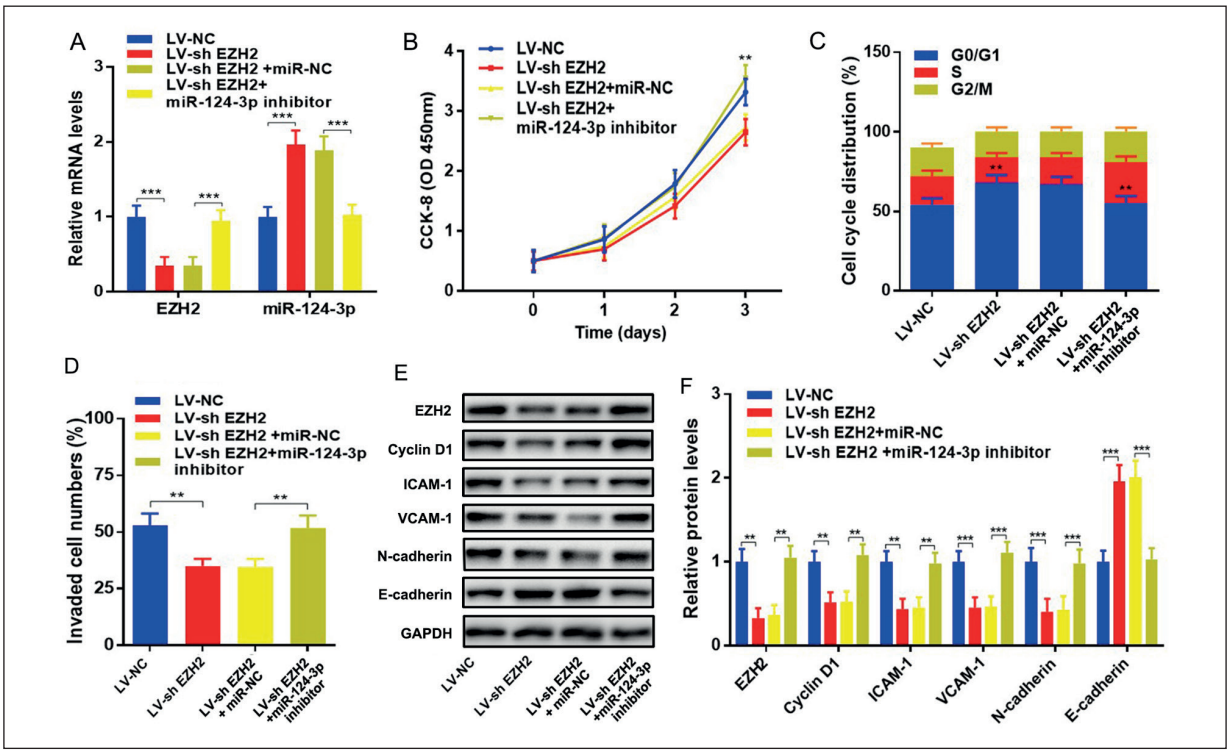

Figure 5. MiR-124-3p/EZH2 axis regulated cell proliferation and invasion in MKN28 cells. **A,** The mRNA expressions of EZH2 and miR-124-3p were detected by RT-PCR. **B,** CCK8 assay was used to measure cell proliferation abilities. **C,** FACS was used to measure cell cycle distribution. **D,** Transwell assay was used to detect cell invasion abilities. **E, F,** Protein expressions of Cyclin D1, ICAM-1, VCAM-1, N-cadherin and E-cadherin were detected by WB (magnifications × 0.8). **p<0.01, ***p<0.001.

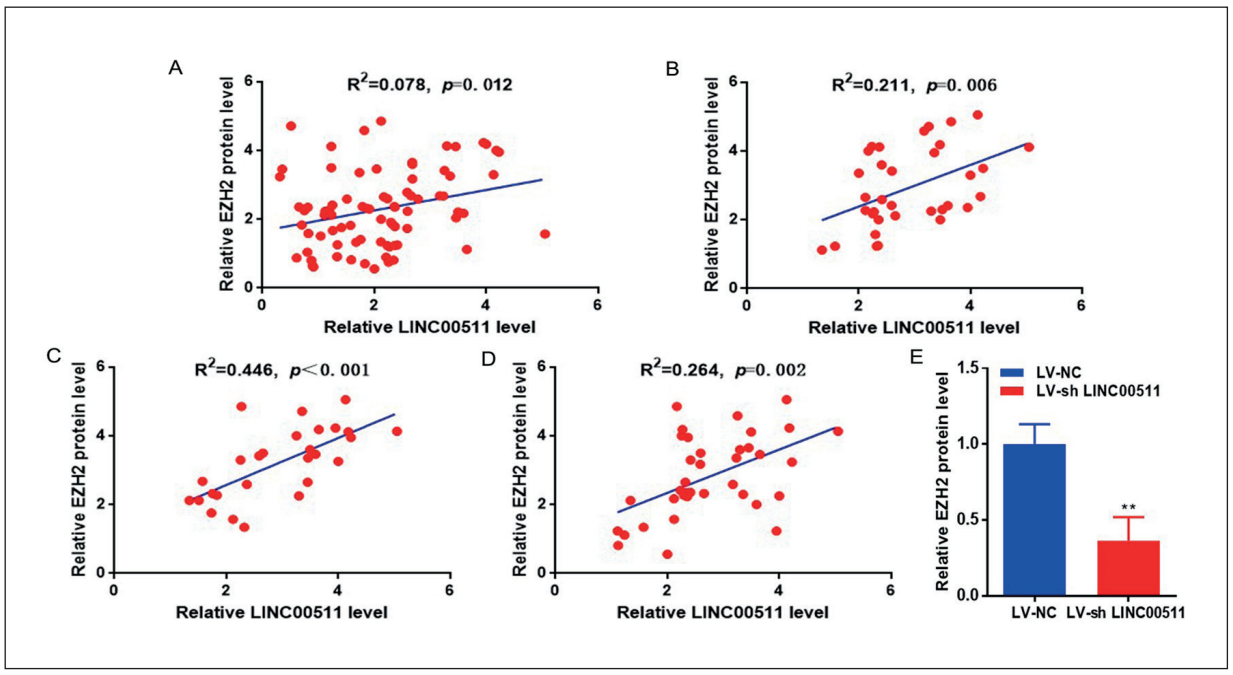

Figure 6. LINC00511 was positively interacted with EZH2. **A,** Correlation between LINC00511 and EZH2 was analyzed in GC patients. **B,** Correlation between LINC00511 and EZH2 was analyzed in GC patients at stage III-IV. **C,** Correlation between LINC00511 and EZH2 was analyzed in tumor size larger than 5 cm. **D,** Correlation between LINC00511 and EZH2 was analyzed in patients with metastasis. **E,** EZH2 protein expressions in LV-sh EZH2 and LV-NC were detected by WB. **p<0.01, ***p<0.001.

acted with EZH2 and we might conclude that LINC00511 could sponge with miR-124-3p, which might then target at repressing EZH2 expression.

LINC00511 Regulated Cell Proliferation and Invasion Via MiR-124-3p/ EZH2 Pathway In GC

To verify our assumption, we added miR-124-3p inhibitor or miR-NC into MKN28 cells with LV-shLINC00511 or LV-NC. Results showed that LINC00511 was reduced in LV-shLINC00511 and it was reversed following with miR-124-3p inhibition (Figure 7A) ($p<0.001$), miR-124-3p was promoted in LV-shLINC00511 and it was reversed following with miR-124-3p inhibition (Figure 7A) ($p<0.001$). Furthermore, CCK-8 assays revealed that cell proliferation ability was inhibited in LV-shLINC00511, while it was promoted following with miR-124-3p inhibitor transfection (Figure 7B) ($p<0.01$). Moreover, FACS assay showed that LINC00511 inhibition repressed cell growth by increasing cell distribution in G0/G1 phase and reducing cell distribution in S phase, while it was reversed following with miR-124-3p inhibition (Figure 7C) ($p<0.01$). Besides, transwell assay illustrated that LINC00511 inhibition repressed cell invasion ability, while it was reversed following with miR-124-3p inhibition (Figure 7D) ($p<0.001$). Additionally, WB showed that LINC00511 inhibition repressed protein expressions of EZH2, Cyclin D1, ICAM-1, VCAM-1, N-cadherin and increased N-cadherin expression, while they were reversed following with miR-124-3p inhibition (Figure 7E, F) ($p<0.01$). Collectively, these results indicated that LINC00511 regulated proliferation and invasion via miR-124-3p/EZH2 axis in GC patients.

Discussion

GC is a malignant cancer with high incidence and mortality in the world[1-3]. Most patients have been diagnosed at later stage or metastasis stage,

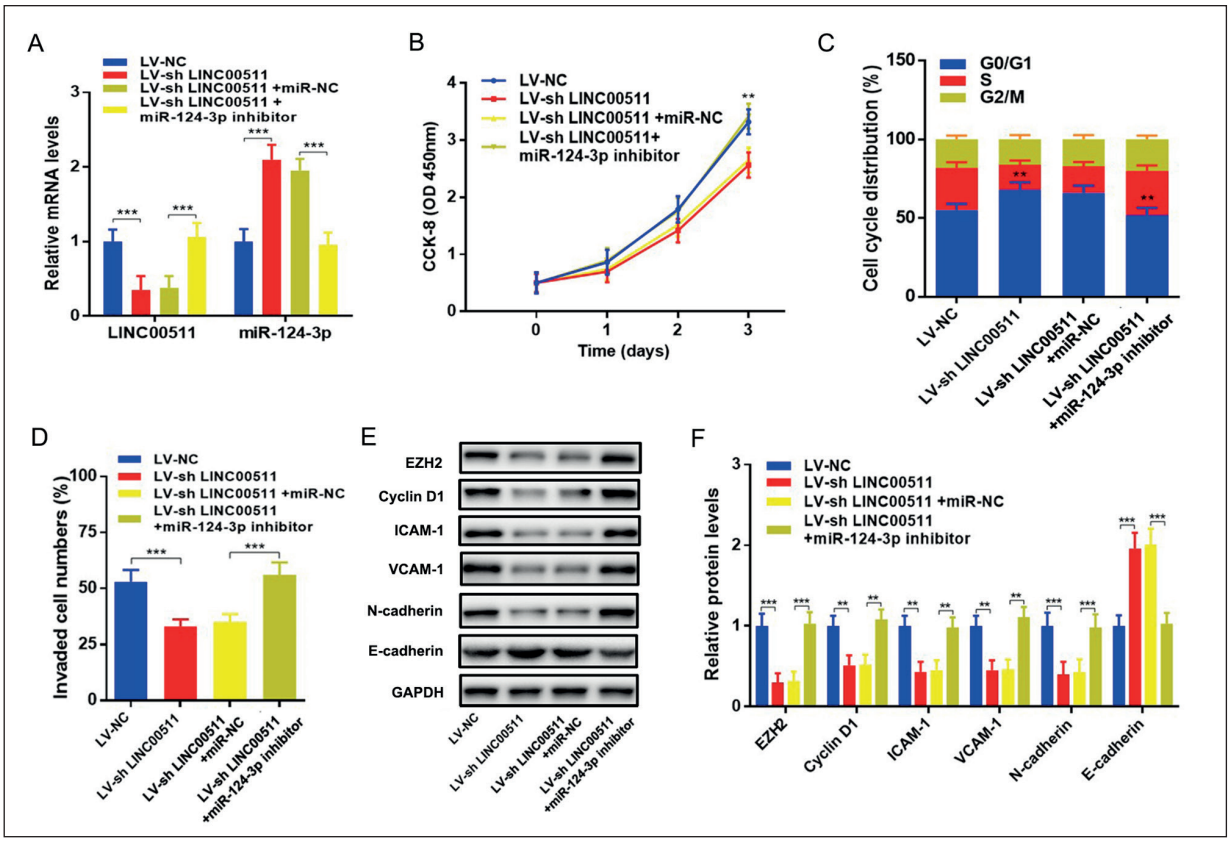

Figure 7. LINC00511 regulated cell proliferation and invasion *via* miR-124-3p/ EZH2 pathway in GC. **A,** The mRNA expressions of LINC00511 and miR-124-3p were detected. **B,** CCK8 assay was used to measure cell proliferation abilities. **C,** FACS was used to measure cell cycle distribution. **D,** Transwell assay was used to detect cell invasion abilities. **E, F,** Protein expressions of EZH2, Cyclin D1, ICAM-1, VCAM-1, N-cadherin and E-cadherin were detected by WB (magnifications × 0.8). $^{**}p<0.01$, $^{***}p<0.001$.

although new surgical treatments, chemotherapy and advanced diagnosis methods have been applied for GC patients, which have already improved the future outcome for patients[1-4]. However, these treatments have limited effects and more novel biomarkers and treatments should be developed to improve the poor future outcome for patients.

LncRNAs have been found to regulate biological features in various diseases and they play important roles in the development of different cancers[9-11], including GC[12-14]. LINC00511 was reported to be an oncogene to promote tumor formation and development in some cancers[15-17]. However, whether LINC00511 plays some roles in GC remained unclear. In this study, for the first time, we detected the expressions of LINC00511 in GC tissues and adjacent normal tissues. We found that LINC00511 was significantly increased in GC tissues, which was correlated with metastasis, tumor size and the poor future diagnosis of GC patients. Furthermore, we also revealed the expressions of LINC00511 in GC cell lines. Results illustrated that LINC00511 was increased in GC cell lines, especially in MKN28 cells. However, the functions and potential mechanisms of LINC00511 in GC remained unknown.

Cyclin D1 is a protein encoded by CCND1 gene, which is indispensable for transiting cells from G1 to S phase and it is associated with cell proliferation in various cancers[34-36]. Intercellular cell adhesion molecule-1 (ICAM-1) and vascular cell adhesion molecule-1 (VCAM-1) are important adhesion molecules to promote cell adhesion and invasion in cancers[37-39]. N-cadherin and E-cadherin are from the cadherin family, which are from the Ca^{2+} dependent cell adhesion molecule family and can promote cell invasion in various cancers[40,41]. Epithelial-mesenchymal transition (EMT) is a biological process by which epithelial cells are transformed into cells with mesenchymal phenotype, the cell adhesion molecules are decreased, such as E-cadherin and the cytokeratin cytoskeleton is transformed into Vimentin-based cytoskeleton[42,43]. Epithelial cells have lost their cell polarity and acquired the ability to migrate and invade during EMT, which is of great significance in the development and metastasis of malignant tumors[42,43], including gastric cancer[44,45].

To find whether LINC00511 could affect cell proliferation and other biological functions, LINC00511 sh-RNA was constructed and infected into MKN28 cells, resulted with LINC00511 inhibition. Results showed that LINC00511 inhibition repressed cell proliferation and invasion abilities, protein levels of Cyclin D1, ICAM-1, VCAM-1 and N-cadherin were repressed as well. These data suggested that LINC00511 knockdown inhibited cell proliferation and invasion in MKN28 cells. However, the detailed mechanism remained unknown.

LncRNAs could function as a competing endogenous RNA (ceRNA) to interact with miRNA and regulate the development of different cancers[22,23]. MiR-124-3p was reported to be a tumor suppressor in several human cancers[26-28] and bioinformatics analysis revealed that miR-124-3p might be a target miRNA for LINC00511. We aimed to verify that LINC00511 regulated cell proliferation and invasion by interacting with miR-124-3p. We detected expressions of miR-124-3p in GC tissues and non-tumor tissues, which revealed that miR-124-3p was repressed in GC tissues, especially in patients at stage III-IV, GC tissues larger than 5 cm and patients with metastasis, which was negatively related with LINC00511. Luciferase reporter assay further proved that LINC00511 could directly bind to miR-124-3p in MKN28 cells.

It was reported that EZH2 was an oncogenic gene to promote tumorigenesis and development in various cancers[31-33]. EZH2 was predicted as a potential target gene by Targetscan database. Then, we detected protein expressions of EZH2 in GC tissues and non-tumor tissues, which revealed that EZH2 was increased in GC tissues, especially in patients at stage III-IV, GC tissues larger than 5 cm and patients with metastasis, which were negatively related with miR-124-3p and positively related with LINC00511. Luciferase reporter assay further proved that miR-124-3p could directly bind to EZH2 in MKN28 cells and regulate cell proliferation and invasion.

To detect that miR-124-3p/EZH2 axis contributed to regulate cell proliferation and invasion of GC, miR-124-3p inhibitor was transfected into MKN28 cells with LV-sh EZH2. Results showed that EZH2 was repressed and miR-124-3p was increased following with LV-sh EZH2 infection, while they were reversed following with miR-124-3p inhibition. We illustrated that EZH2 inhibition repressed cell proliferation and invasion capacities, while they were reversed following with miR-124-3p inhibition. These data suggested that miR-124-3p/EZH2 axis regulated cell proliferation and invasion in MKN28 cells.

We might conclude that LINC00511 could sponge with miR-124-3p, which would then target at repressing EZH2 expression and regulate the biological functions of GC. To verify our assumption, we added miR-124-3p inhibitor or miR-NC into MKN28 cells with LV-shLINC00511 or LV-NC. Results showed that LINC00511 inhibition repressed cell proliferation and invasion capacities, while they were reversed following with miR-124-3p inhibition. Taken together, these data suggested that LINC00511 regulated cell proliferation and invasion *via* miR-124-3p/EZH2 axis in GC.

In this work, for the first time, we found that LINC00511 was upregulated in human GC tissues, which might be used as a marker for GC. Moreover, we demonstrated that LINC00511 had the capacities of promoting cell proliferation and invasion through sponging with miR-124-3p/EZH2 axis, which was a novel signaling pathway in GC so far. This study might provide a new insight for the development and treatment of GC.

Conclusions

Above all, this investigation demonstrated that LINC00511 was increased in GC tissues, which was associated with the poor OS in patients with GC. We uncovered a previously unappreciated LINC00511/miR-124-3p/EZH2 signaling axis in promoting cell proliferation and invasion in GC patients and GC cell lines, which suggested that it might be a potential target for treating human GC.

Conflict of Interest

The Authors declare that they have no conflict of interests.

References

1) Chen W. Cancer statistics: updated cancer burden in China. Chin J Cancer Res 2015; 27: 1.
2) Chen W, Zheng R, Baade PD, Zhang S, Zeng H, Bray F, Jemal A, Yu XQ, He J. Cancer statistics in China, 2015. CA Cancer J Clin 2016; 66: 115-132.
3) Siegel RL, Miller KD, Jemal A. Cancer statistics, 2019. CA Cancer J Clin 2019; 69: 7-34.
4) Feng RM, Zong YN, Cao SM, Xu RH. Current cancer situation in China: good or bad news from the 2018 Global Cancer Statistics? Cancer Commun (Lond) 2019; 39: 22.
5) Chen K, Xie S, Jin W. Crucial lncRNAs associated with adipocyte differentiation from human adipose-derived stem cells based on co-expression and ceRNA network analyses. PeerJ 2019; 7: e7544.
6) Cheng JT, Wang L, Wang H, Tang FR, Cai WQ, Sethi G, Xin HW, Ma Z. Insights into biological role of lncrnas in epithelial-mesenchymal transition. Cells 2019; 8: pii: E1178.
7) Guo X, Wang J, Chen J. Identification of aberrantly expressed lncRNAs involved in orthodontic force using a subpathway strategy. Comput Math Methods Med 2019; 2019: 9250129.
8) Hong S, Hu S, Kang Z, Liu Z, Yang W, Zhang Y, Yang D, Ruan W, Yu G, Sun L, Chen L. Identification of functional lncRNAs based on competing endogenous RNA network in osteoblast differentiation. J Cell Physiol 2020; 235: 2232-2244.
9) Qi L, Zhang T, Yao Y, Zhuang J, Liu C, Liu R, Sun C. Identification of lncRNAs associated with lung squamous cell carcinoma prognosis in the competitive endogenous RNA network. PeerJ 2019; 7: e7727.
10) Sun Z, Zhang C, Wang T, Shi P, Tian X, Guo Y. Correlation between long non-coding RNAs lncRNAs) H19 expression and trastuzumab resistance in breast cancer. J Cancer Res Ther 2019; 15: 933-940.
11) Zhu J, Chen S, Yang B, Mao W, Yang X, Cai J. Molecular mechanisms of lncRNAs in regulating cancer cell radiosensitivity. Biosci Rep 2019; 39. pii: BSR20190590
12) Dong XZ, Zhao ZR, Hu Y, Lu YP, Liu P, Zhang L. LncRNA COL1A1-014 is involved in the progression of gastric cancer via regulating CXCL12-CXCR4 axis. Gastric Cancer 2020; 23: 260-272. 13) Xiao J, Lai H, Wei SH, Ye ZS, Gong FS, Chen LC. lncRNA HOTAIR promotes gastric cancer proliferation and metastasis via targeting miR-126 to active CXCR4 and RhoA signaling pathway. Cancer Med 2019; 8: 6768-6779.
14) Zhang P, Li S, Chen Z, Lu Y, Zhang H. LncRNA SNHG8 promotes proliferation and invasion of gastric cancer cells by targeting the miR-491/PDGFRA axis. Hum Cell 2020; 33: 123-130.
15) Deng H, Huang C, Wang Y, Jiang H, Peng S, Zhao X. LINC00511 promotes the malignant phenotype of clear cell renal cell carcinoma by sponging microRNA-625 and thereby increasing cyclin D1 expression. Aging (Albany NY) 2019; 11: 5975-5991.
16) Lu G, Li Y, Ma Y, Lu J, Chen Y, Jiang Q, Qin Q, Zhao L, Huang Q, Luo Z, Huang S, Wei Z. Long noncoding RNA LINC00511 contributes to breast cancer tumourigenesis and stemness by inducing the miR-185-3p/E2F1/Nanog axis. J Exp Clin Cancer Res 2018; 37: 289.
17) Yu CL, Xu XL, Yuan F. LINC00511 is associated with the malignant status and promotes cell proliferation and motility in cervical cancer. Biosci Rep 2019; 39. pii: BSR20190903
18) Bartel DP. MicroRNAs: target recognition and regulatory functions. Cell 2009; 13: 215-233.

19) Fang C, Li Y. Prospective applications of microRNAs in oral cancer. Oncol Lett 2019; 18: 3974-3984.

20) Qiao J, Du Y, Yu J, Guo J. MicroRNAs as potential biomarkers of insecticide exposure: a review. Chem Res Toxicol 2019; 32: 2169-2181.

21) Rahman MM, Brane AC, Tollefsbol TO. MicroRNAs and Epigenetics strategies to reverse breast cancer. Cells 2019; 8. pii: E1214.

22) Salmena L, Poliseno L, Tay Y, Kats L, Pandolfi PP. A ceRNA hypothesis: the Rosetta Stone of a hidden RNA language? Cell 2011; 146: 353-358.

23) Tay Y, Kats L, Salmena L, Weiss D, Tan SM, Ala U, Karreth F, Poliseno L, Provero P, Di Cunto F, Lieberman J, Rigoutsos I, Pandolfi PP. Coding-independent regulation of the tumor suppressor PTEN by competing endogenous mRNAs. Cell 2011; 147: 344-357.

24) Liang W, Sun F. Identification of pivotal lncRNAs in papillary thyroid cancer using lncRNA-mRNA-miRNA ceRNA network analysis. PeerJ 2019; 7: e7441.

25) Song X, Zhang C, Liu Z, Liu Q, He K, Yu Z. Characterization of ceRNA network to reveal potential prognostic biomarkers in triple-negative breast cancer. PeerJ 2019; 7: e7522.

26) Fu W, Wu X, Yang Z, Mi H. The effect of miR-124-3p on cell proliferation and apoptosis in bladder cancer by targeting EDNRB. Arch Med Sci 2019; 15: 1154-1162.

27) Lv Y, Chen S, Wu J, Lin R, Zhou L, Chen G, Chen H, Ke Y. Upregulation of long non-coding RNA OGFRP1 facilitates endometrial cancer by regulating miR-124-3p/SIRT1 axis and by activating PI3K/AKT/GSK-3beta pathway. Artif Cells Nanomed Biotechnol 2019; 47: 2083-2090.

28) Yan G, Li Y, Zhan L, Sun S, Yuan J, Wang T, Yin Y, Dai Z, Zhu Y, Jiang Z, Liu L, Fan Y, Yang F, Hu W. Decreased miR-124-3p promoted breast cancer proliferation and metastasis by targeting MGAT5. Am J Cancer Res 2019; 9: 585-596.

29) Li H, Xie S, Liu M, Chen Z, Liu X, Wang L, Li D, Zhou Y. The clinical significance of downregulation of mir-124-3p, mir-146a-5p, mir-155-5p and mir-335-5p in gastric cancer tumorigenesis. Int J Oncol 2014; 4: 197-208.

30) Liu F, Hu H, Zhao J, Zhang Z, Ai X, Tang L, Xie L. MiR-124-3p acts as a potential marker and suppresses tumor growth in gastric cancer. Biomed Rep 2018, 9: 147-155.

31) Liu Z, Yang L, Zhong C, Zhou L. EZH2 regulates H2B phosphorylation and elevates colon cancer cell autophagy. J Cell Physiol 2020; 235: 1494-1503.

32) Roh JW, Choi JE, Han HD, Hu W, Matsuo K, Nishimura M, Lee JS, Kwon SY, Cho CH, Kim J, Coleman RL, Lopez-Bernstein G, Sood AK. Clinical and biological significance of EZH2 expression in endometrial cancer. Cancer Biol Ther 2019; 21: 147-156.

33) Wang FW, Ao X, Fu SM. The functional role of the EZH2 gene in controlling breast cancer stem cells. J BUON 2019; 24: 1060-1066.

34) Holah NS, Hemida AS. Cyclin D1 and PSA act as good prognostic and clinicopathological indicators for breast cancer. J Immunoassay Immunochem 2020: 41: 28-44.

35) Ramos-García P, González-Moles MÁ, González-Ruiz L, Ayén Á, Ruiz-Ávila I, Bravo M, Gil-Montoya JA. Clinicopathological significance of tumor cyclin D1 expression in oral cancer. Arch Oral Biol 2019; 99: 177-182.

36) Zhong Q, Hu Z, Li Q, Yi T, Li J, Yang H. Cyclin D1 silencing impairs DNA double strand break repair, sensitizes BRCA1 wildtype ovarian cancer cells to olaparib. Gynecol Oncol 2019; 152: 157-165.

37) Chen M, Peng W, Hu S, Deng J. MiR-126/VCAM-1 regulation by naringin suppresses cell growth of human non-small cell lung cancer. Oncol Lett 2018; 16: 4754-4760.

38) Kawczyk-Krupka A, Czuba ZP, Kwiatek B, Kwiatek S, Krupka M, SieroĐ K. The effect of ALA-PDT under normoxia and cobalt chloride CoCl2-induced hypoxia on adhesion molecules ICAM-1, VCAM-1) secretion by colorectal cancer cells. Photodiagnosis Photodyn Ther 2017; 19: 103-115.

39) Reina M, Espel E. Role of LFA-1 and ICAM-1 in cancer. Cancers (Basel) 2017; 9. pii: E153.

40) Cao ZQ, Wang Z, Leng P. Aberrant N-cadherin expression in cancer. Biomed Pharmacother 2019; 118: 109320.

41) Labernadie A, Kato T, Brugués A, Serra-Picamal X, Derzsi S, Arwert E, Weston A, González-Tarragó V, Elosegui-Artola A, Albertazzi L, Alcaraz J, Roca-Cusachs P, Sahai E, Trepat X. A mechanically active heterotypic E-cadherin/N-cadherin adhesion enables fibroblasts to drive cancer cell invasion. Nat Cell Biol 2017; 19: 224-237.

42) Cho ES, Kang HE, Kim NH, Yook JI. Therapeutic implications of cancer epithelial-mesenchymal transition (EMT). Arch Pharm Res 2019; 42: 14-24.

43) George JT, Jolly MK, Xu S, Somarelli JA, Levine H. Survival outcomes in cancer patients predicted by a partial emt gene expression scoring metric. Cancer Res 2017; 77: 6415-6428.

44) Xia Y, Wang L, Xu Z, Kong R, Wang F, Yin K, Xu J, Li B, He Z, Wang L, Xu H, Zhang D, Yang L, Wu JY, Xu Z. Reduced USP33 expression in gastric cancer decreases inhibitory effects of Slit2-Robo1 signalling on cell migration and EMT. Cell Prolif 2019; 52: e12606.

45) Yan K, Tian J, Shi W, Xia H, Zhu Y. LncRNA SNHG6 is associated with poor prognosis of gastric cancer and promotes cell proliferation and EMT through epigenetically silencing p27 and sponging miR-101-3p. Cell Physiol Biochem 2017; 42: 999-1012.